



# Electronic structure, electron–phonon coupling and superconductivity of isotypic noncentrosymmetric crystals $\text{Li}_2\text{Pd}_3\text{B}$ and $\text{Li}_2\text{Pt}_3\text{B}$

S.K. Bose \*, E.S. Zijlstra

*Physics Department, Brock University, 500 Glenridge Avenue, St. Catharines, Ont., Canada L2S 3A1*

Received 14 July 2005; accepted 5 August 2005

Available online 27 September 2005

## Abstract

Electronic structure of recently discovered isotypic ternary borides  $\text{Li}_2\text{Pd}_3\text{B}$  and  $\text{Li}_2\text{Pt}_3\text{B}$ , with noncentrosymmetric crystal structures, is studied with a view to understanding their superconducting properties. Estimates of the Fermi surface averaged electron–phonon matrix element and Hopfield parameter are obtained in the rigid ion approximation of Gaspari and Gyorffy [G.D. Gaspari, B.L. Gyorffy, *Phys. Rev. Lett.* 28 (1972) 801]. The contribution of the lithium atoms to the electron–phonon coupling is found to be negligible, while both boron and palladium atoms contribute equally strongly to the Hopfield parameter. There is a significant transfer of charge from lithium, almost the entire valence charge, to the B–Pd(Pt) complex. The electronic structure and superconducting properties of  $\text{Li}_2\text{Pd}_3\text{B}$ , thus, can be understood from the viewpoint of the compound being composed of a connected array of B–Pd tetrahedra decoupled from the backbone of Li atoms, which are connected by relatively short bonds. Our results suggest that conventional s-wave electron–phonon interaction without explicit consideration of SO coupling can explain qualitatively the observed  $T_c$  in  $\text{Li}_2\text{Pd}_3\text{B}$ . However, such an approach is likely to fail to describe superconductivity in  $\text{Li}_2\text{Pt}_3\text{B}$ .

© 2005 Elsevier B.V. All rights reserved.

*PACS:* 74.70.–b; 74.62.Fj; 74.25.Kc; 71.20.–b

*Keywords:* Electron–phonon coupling; Hopfield parameter; Rigid ion and muffin-tin approximations; Linear muffin-tin orbitals

## 1. Introduction

The recently synthesized isotypic metal-rich ternary borides  $\text{Li}_2\text{Pd}_3\text{B}$  and  $\text{Li}_2\text{Pt}_3\text{B}$  [1], with noncentrosymmetric crystal structures, have received

\* Corresponding author. Tel.: +1 905 688 5550/+1 905 688 3876; fax: +1 905 984 4867.

*E-mail address:* [sbose@brocku.ca](mailto:sbose@brocku.ca) (S.K. Bose).

considerable attention because of their superconducting properties [2,3,5,4,6,7]. The superconducting transition temperature  $T_c$  of  $\text{Li}_2\text{Pd}_3\text{B}$  is about 8 K, while its isotypic Pt-based counterpart  $\text{Li}_2\text{Pt}_3\text{B}$  shows a  $T_c$  between 2 and 3 K [8]. Badica et al. [8] have been able to synthesize a series of pseudo-binary solid solutions  $\text{Li}_2\text{B}(\text{Pd}_{1-x}\text{Pt}_x)_3$  with  $x$  varying from 0 to 1 and they report having observed superconductivity in the entire  $x$ -range.  $T_c$  decreases monotonically from  $\sim 8$  K as  $x$  increases from 0, dropping to 2.2–2.8 K for  $x = 1$ . The electronic structure of the two end compounds of the solid solution  $\text{Li}_2\text{Pd}_3\text{B}$  and  $\text{Li}_2\text{Pt}_3\text{B}$  have been discussed by Chandra et al. [4]. Sardar and Sa [5] have used a three-dimensional single band  $t$ - $J$  model to discuss the superconductivity of  $\text{Li}_2\text{Pd}_3\text{B}$ , pointing out that the superconductivity in this compound arises from the Pd 4d electrons, and thus should be dominated by the strong correlation effects of narrow band Pd 4d electrons. The importance of the correlation effects of the 4d electrons for the superconducting properties of  $\text{Li}_2\text{Pd}_3\text{B}$  and  $\text{Li}_2\text{Pt}_3\text{B}$  was also mentioned by Chandra and Mathi [4]. On the other hand, Yokoya et al. [7] report excellent agreement between their X-ray photoemission results for the valence band spectrum and standard band structure calculations, which can describe only weakly correlated materials. They conclude that the correlation effects play a negligible role for the physical properties of this superconductor, and that superconductivity in this material arises from the Pd 4d electrons hybridized with B 2p and Li 2p electrons. Absence of strong correlation effects in  $\text{Li}_2\text{Pd}_3\text{B}$  is also indicated in the  $^{11}\text{B}$  NMR measurements in this compound by Nishiyama et al. [6]. Since the Pd(Pt) bands are almost full [4], the correlation effects are not expected to be strong. The purpose of the present work is to examine the two isotypic superconductors  $\text{Li}_2\text{Pd}_3\text{B}$  and  $\text{Li}_2\text{Pt}_3\text{B}$  from the viewpoint of electron–phonon coupling and conventional (s-wave) superconductivity, without explicit consideration of electron correlation effects and spin–orbit (SO) coupling. To this end, we use the rigid muffin-tin approach of Gaspari and Gyorffy [9] implemented within the linear muffin-tin orbital (LMTO) method [10] by Glötzel et al. [11] and later by Skriver and Mertig [12].

The present paper is organized as follows. In Section 2 we discuss the electronic structure, charge transfer and bonding in the two compounds. In Section 3 we discuss the electron–phonon coupling. In particular we provide estimates of the Fermi surface averaged electron–phonon matrix elements (Hopfield parameters), and electron–phonon coupling constants. Our results indicate that conventional electron–phonon coupling, without consideration of SO effects, can describe the observed superconductivity in  $\text{Li}_2\text{Pd}_3\text{B}$ , but not in  $\text{Li}_2\text{Pt}_3\text{B}$ . There is some similarity in the superconducting properties of  $\text{Li}_2\text{Pt}_3\text{B}$  and another recently discovered noncentrosymmetric crystal  $\text{CePt}_3\text{Si}$  with strong SO coupling [13]. This is discussed in Section 3. In Section 4 we present our conclusions.

## 2. Electronic structure

The electronic structures of the two ternary borides  $\text{Li}_2\text{Pd}_3\text{B}$  and  $\text{Li}_2\text{Pt}_3\text{B}$ , which crystallize in the  $\text{P4}_332$  structure (space group no. 212) with 4 formula units per unit cell [1], were calculated with the LMTO [10] method using the atomic sphere

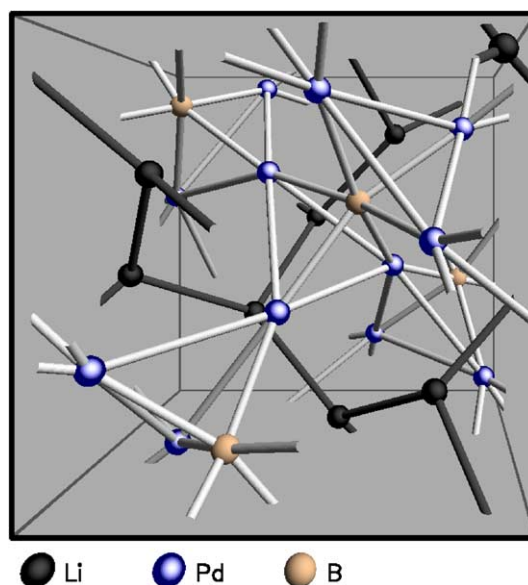


Fig. 1. Unit cell of  $\text{Li}_2\text{Pd}_3\text{B}$ .

approximation (ASA). The lattice constants used were  $12.762$  and  $12.765a_0$  for  $\text{Li}_2\text{Pd}_3\text{B}$  and  $\text{Li}_2\text{Pt}_3\text{B}$ , respectively. The positions of the atoms were taken to be the same as given by Eibenstein and Jung [1] and used in the electronic structure calculation of Chandra et al. [4]. The atomic structure is shown in Fig. 1. The shortest bonds are between Pd and B ( $4.0a_0$ ) and Li and Li ( $4.8a_0$ ). Each B atom is connected to six Pd atoms, and each Pd atom has two B nearest neighbors. The structure of the Pd and B atoms can be described as a network of connected  $\text{Pd}_3\text{B}$  tetrahedra [4]. To show this, in Fig. 1 we have also drawn bonds for the shortest Pd–Pd distances ( $5.3a_0$ ), which are however longer than some of the Pd–Li distances ( $5.2a_0$ , not shown). The threefold coordinated Li

atoms form their own network (Fig. 1). Because the Li–Li distances are 16% smaller than in bcc Li [5], it has been anticipated [5] that the Li atoms transfer their 2s electrons entirely to the Pd and B atoms. The valence charge density of  $\text{Li}_2\text{Pd}_3\text{B}$  [Fig. 2(b)], the total charge density is presented in Fig. 2(a)], shows indeed that there is very little electronic valence charge present near the Li atoms. To see the effect of bonding it is often useful to subtract the atomic valence charge densities from the total valence charge density. The result is shown in Fig. 3. Again it is clear that the network of Li atoms is depleted of charge. In addition, a strong increase in the charge density is found between the B and Pd atoms, which indicates covalent bonding. The increase in charge density

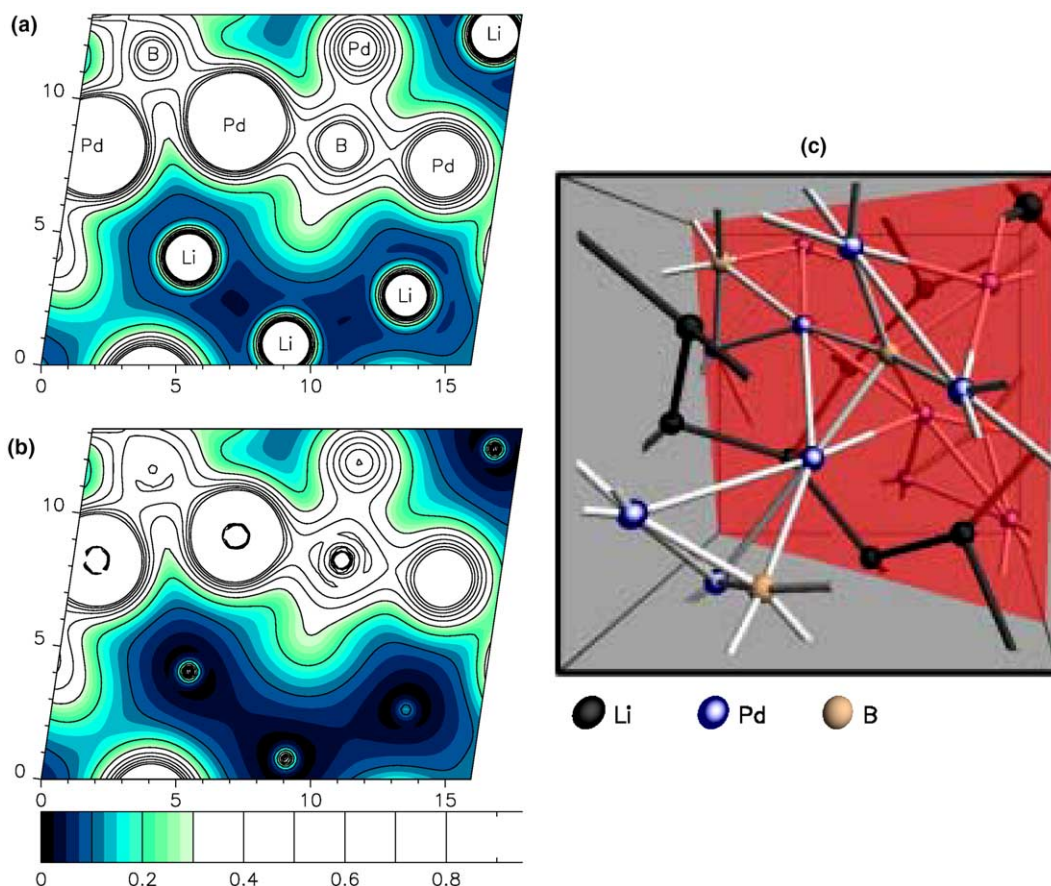


Fig. 2. (a) Total and (b) valence charge densities of  $\text{Li}_2\text{Pd}_3\text{B}$  in (c) the plane that passes through the points  $(0,0,0)$ ,  $(a/4,0,a)$ , and  $(a,a,a)$ .

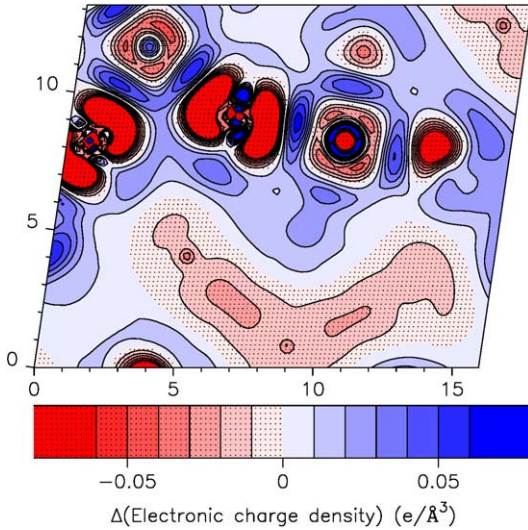


Fig. 3. Difference of the valence charge density of  $\text{Li}_2\text{Pd}_3\text{B}$  and a superposition of atomic valence charge densities.

between the Pd atoms is less pronounced, suggesting that B–Pd bonds are stronger than Pd–Pd bonds.

We have carried out the LMTO calculation without empty spheres (which a more rigorous calculation would have required) using the spdf basis and with the f-orbitals downfolded. Even though our results are not the best possible results within the LMTO–ASA scheme, a comparison with more rigorous full-potential linear augmented plane waves plus local orbitals (FP-LAPW + lo) results presented by Chandra et al. [4] shows that our results are of acceptable accuracy. The densities of states shown in Fig. 4 agree very well with the results of Chandra et al. [4]. The agreement of our calculated densities of states with another set of FP-LAPW results of Yokoya et al. [7] is also very good. In Fig. 4 among the various partial densities of states, only the Pd(Pt)-d and B-p densities of states are shown, since these have the largest values at the Fermi level and as a result electron–phonon interaction is dominated by Pd(Pt) d–f and B p–d scattering (Section 3). Note that the density of states per atom is almost the same for Pd-d (3.34 States/(Ry atom)) and B-p states (3.23 States/(Ry atom)) in  $\text{Li}_2\text{Pd}_3\text{B}$ . In  $\text{Li}_2\text{Pt}_3\text{B}$  these numbers corresponding to Pt-d and B-p states are 4.2 States/(Ry atom) and 3.72 States/(Ry atom), respectively.

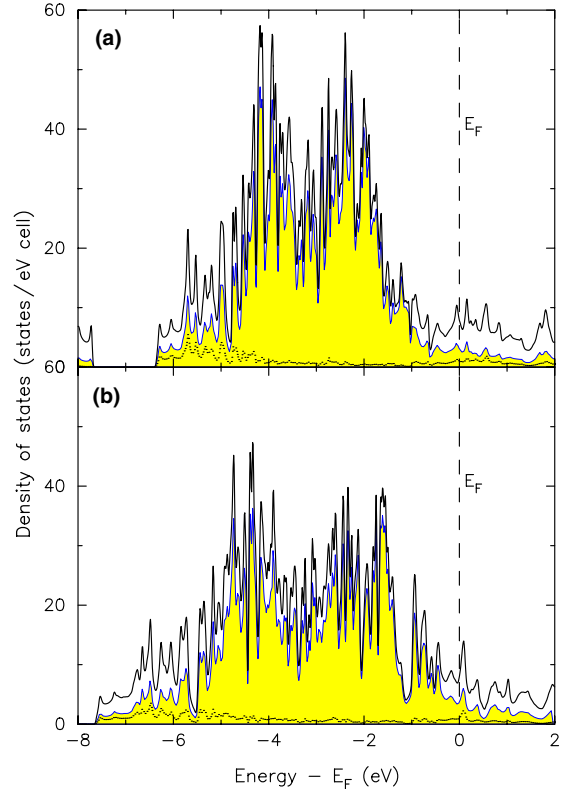


Fig. 4. Densities of states of (a)  $\text{Li}_2\text{Pd}_3\text{B}$  and (b)  $\text{Li}_2\text{Pt}_3\text{B}$  (thick solid curves). Partial Pd and Pt-d (thin curves, shadings) and B-p (dotted curves) densities of states are also shown.

The main features of our LMTO calculations that are used in estimating the electron–phonon matrix elements in Section 3 are the atom and orbital resolved densities of states, listed in Table 1. In addition, the potentials at the sphere boundaries and LMTO potential parameters calculated with the LMTO reference energies set at the Fermi energy also enter the expression for the electron–phonon matrix elements, as discussed in Section 3.

### 3. Electron–phonon coupling and superconductivity

According to McMillan’s strong coupling theory [14] the electron–phonon coupling constant  $\lambda_{e-ph}$  for a one-component system, i.e. elemental solid, can be written as

Table 1

Partial  $l$  and atom resolved densities of states, including both spins, at the Fermi energy in states/Ry for 24 atom unit cells of  $\text{Li}_2\text{Pd}_3\text{B}$  and  $\text{Li}_2\text{Pt}_3\text{B}$

Compound	Atom	$n_s$	$n_p$	$n_d$	$n_f$
$\text{Li}_2\text{Pd}_3\text{B}$	Pd	7.132	18.54	40.12	1.162
	Li	6.000	11.53	2.566	0.481
	B	0.887	12.92	1.084	0.333
$\text{Li}_2\text{Pt}_3\text{B}$	Pt	7.499	17.38	50.47	1.980
	Li	3.284	6.791	2.586	0.709
	B	0.837	14.89	1.093	0.361

The numbers shown are for 12 Pd(Pt), 8 Li and 4 B atoms. The total Fermi level DOS,  $n(E_F)$ , is 102.75 states/Ry/cell for  $\text{Li}_2\text{Pd}_3\text{B}$  and 107.8 states/Ry/cell for  $\text{Li}_2\text{Pt}_3\text{B}$ .

$$\lambda_{\text{e-ph}} = \frac{n(E_F)\langle I^2 \rangle}{M\langle \omega^2 \rangle}, \quad (1)$$

where  $M$  is the atomic mass,  $\langle \omega^2 \rangle$  is the renormalized phonon frequency, squared and averaged according to the prescriptions in Ref. [14],  $n(E_F)$  is the density of states for one type of spin at the Fermi energy  $E_F$ , and  $\langle I^2 \rangle$  is the square of the electron–phonon matrix element averaged over the Fermi surface. Gaspari and Gyorffy [9] constructed a theory to calculate the quantity  $\langle I^2 \rangle$  on the assumption that the additional scattering of an electron caused by the displacement of an atom (ion) is dominated by the change in the local potential. Within the rigid muffin-tin approximation used by Gaspari and Gyorffy [9] the spherically averaged part of the Hopfield parameter  $\eta = n(E_F)\langle I^2 \rangle$  can be written as (in atomic Rydberg units)

$$\eta = 2n(E_F) \sum_l (l+1) M_{l,l+1}^2 \frac{f_l}{2l+1} \frac{f_{l+1}}{2l+3}, \quad (2)$$

where  $f_l$  is a relative partial state density,

$$f_l = \frac{n_l(E_F)}{n(E_F)} \quad (3)$$

and  $M_{l,l+1}$  is the electron–phonon matrix element obtained from the gradient of the potential and the radial solutions  $R_l$  and  $R_{l+1}$  of the Schrödinger equation evaluated at the Fermi energy. Gaspari and Gyorffy [9] derived an expression for  $M_{l,l+1}$  using the rigid muffin-tin approximation in terms of partial wave phase shifts. Glötzel et al. [11] and Skriver and Mertig [12], using the LMTO

[10] method, expressed this quantity in terms of the logarithm derivative  $D_l(E_F)$  of the radial solution at the sphere boundary, with the reference energy  $E_v$  set at the Fermi energy  $E_F$ :

$$M_{l,l+1} = -\phi_l(E_F)\phi_{l+1}(E_F)\{[D_l(E_F) - l][D_{l+1}(E_F) + l + 2] + [E_F - V(S)]S^2\}, \quad (4)$$

where  $S$  is the sphere radius,  $V(S)$  is the one-electron potential and  $\phi_l(E_F)$  the sphere-boundary amplitude of the  $l$  partial wave evaluated at the Fermi level.

The extension of the Gaspari and Gyorffy scheme [9] to alloys has been discussed by several authors [15–21]. To obtain an estimate of the Hopfield parameter and gain some insight into electron–phonon coupling in the two isotopic compounds of interest, in this paper we adopt the following simplified approach. Since  $\langle I^2 \rangle$ , in the rigid muffin-tin or rigid atomic sphere approximation, is an atomic quantity, it can be calculated for each atom in the alloy using the formula given by Skriver and Mertig [12], by considering atom-resolved partial densities of states. For atom  $A$

$$\langle I_A^2 \rangle = 2 \sum_l (l+1) M_{(A,(l,l+1))}^2 \frac{f_l^A}{2l+1} \frac{f_{l+1}^A}{2l+3}, \quad (5)$$

where  $f_l^A = \frac{n_l^A(E_F)}{n(E_F)}$ . If there are  $N_A$  atoms of type  $A$  in the unit cell, then  $n(E_F) = \sum_{A,l} N_A n_l^A(E_F)$  and the Hopfield parameter  $\eta$  can be calculated from

$$\eta = \sum_A \eta_A = n(E_F) \sum_A N_A \langle I_A^2 \rangle, \quad (6)$$

an expression, which is independent of the size of the unit cell chosen. This expression ignores possible contribution from cross terms involving more than one atom. The quantities  $M_{(A,(l,l+1))}^2$  can be calculated from the sphere-boundary potentials and the LMTO–ASA potential parameters evaluated with the reference energies set equal to the Fermi energy.

The values for the total and partial densities of states for  $\text{Li}_2\text{Pd}_3\text{B}$  and  $\text{Li}_2\text{Pt}_3\text{B}$  are shown in Table 1. In Table 2 the atom-resolved and the total Hopfield parameters,  $\eta_A$  and  $\eta$ , obtained by using Eqs. (5) and (6) are listed. We also list the calculated bulk moduli of the two compounds, which can be used to obtain estimates of the Debye

Table 2

Bulk modulus  $B$  in GPa, Debye temperature  $\Theta_D$  in K, atom-resolved and total Hopfield parameters given by Eqs. (5) and (6) in  $\text{eV}/\text{\AA}^2$  for  $\text{Li}_2\text{Pd}_3\text{B}$  and  $\text{Li}_2\text{Pt}_3\text{B}$

Compound	$B$	$\Theta_D$	$\eta_{\text{Pd}}$	$\eta_{\text{B}}$	$\eta_{\text{Li}}$	$\eta$
$\text{Li}_2\text{Pd}_3\text{B}$	166	371	1.30	1.10	0.19	2.59
$\text{Li}_2\text{Pt}_3\text{B}$	196	303	2.67	3.69	0.08	6.44

$\eta$  denotes the total Hopfield parameter.

temperatures and average phonon frequencies for these solids. The analysis of the electron–phonon coupling and critical temperatures in the two compounds is based on the quantities listed in Tables 1 and 2.

### 3.1. $\text{Li}_2\text{Pd}_3\text{B}$

For  $\text{Li}_2\text{Pd}_3\text{B}$  the Hopfield parameter calculated according to Eqs. (5) and (6) is  $2.59 \text{ eV}/\text{\AA}^2$ . Note that the boron contribution is only 15% less than the palladium contribution. Most dominant contributions come from Pd d–f ( $0.98 \text{ eV}/\text{\AA}^2$ ) and B p–d ( $0.65 \text{ eV}/\text{\AA}^2$ ) scattering. Although double in number than the B atoms, all Li atoms together contribute only 7% to the Hopfield parameter  $\eta$ . 95% of the contribution of the Li atoms is from the s–p channel.

A few comments regarding the decomposition of the Hopfield parameter into atom-resolved parts and various partial wave channels in an alloy are in order. Because certain potential parameters depend on the ratio  $s/W$  (or  $(s/W)^{2l+1}$ ), where  $s$  is the sphere radius for the atom and  $W$  is the average Wigner–Seitz radius of the alloy, the atom-resolved parameters may differ for different choices of the sphere radii, all chosen within the allowable sphere overlaps. The total Hopfield parameter is expected to be independent of the choice of the sphere radii, if these are chosen to keep the ASA errors as small as possible, but the partial-wave resolved parameters (i.e. s–p, p–d etc.) are dependent on the ratio  $s/W$ . Ideally, the LMTO calculation for the two solids  $\text{Li}_2\text{Pd}_3\text{B}$  and  $\text{Li}_2\text{Pt}_3\text{B}$  should have been carried out with empty spheres in order to reduce ASA errors. This would have given an improved value of the total Hopfield parameter, including contributions from both atomic and empty spheres. Despite some ASA errors present

in our results, we expect the trends revealed by them to be correct.

In the simplest approximation, assuming isotropic electron–phonon coupling, one can attempt to estimate  $\lambda_{\text{e-ph}}$  from  $\eta$  using Eq. (1), assuming that  $M$  is the concentration average of the mass of the component atoms in the alloy and  $\omega$  is the average phonon frequency for the alloy. To estimate the average phonon frequency we use the prescription of Moruzzi et al. [23], relating the Debye temperature  $\Theta_D$  to the bulk modulus, atomic mass and the average Wigner–Seitz radius:

$$\Theta_D = 41.63 \sqrt{\frac{r_0 B}{M}}, \quad (7)$$

where  $r_0$  is the average Wigner–Seitz radius in atomic units,  $B$  is the bulk modulus in kbar and  $M$  is the atomic mass. Although Moruzzi et al. [23] verified the validity of this expression for elemental metallic solids, we assume its validity for the alloy by considering  $M$  to be the concentration average of the masses of the component atoms. From the LMTO calculation of total energy versus volume we find the bulk modulus  $B$  of  $\text{Li}_2\text{Pd}_3\text{B}$  to be 166 GPa, a value consistent with the bulk moduli of elemental solids Pd ( $B = 180.8 \text{ GPa}$ ), B ( $B = 178 \text{ GPa}$ ) and Li ( $B = 11.6 \text{ GPa}$ ) [24]. Using 166 GPa for  $B$  in the above equation we find  $\Theta_D = 371 \text{ K}$ . Using the empirical estimate  $\sqrt{\langle \omega^2 \rangle} = 0.69 \Theta_D$  [12] yields an average phonon frequency of 5.3 THz. The use of Eq. (1) then yields  $\lambda_{\text{e-ph}} = 0.39\text{--}0.4 \text{ K}$ , a value not large enough to explain the observed superconductivity of  $\text{Li}_2\text{Pd}_3\text{B}$  at  $\sim 8 \text{ K}$ . This could have been foreseen from the small value,  $2.59 \text{ eV}/\text{\AA}^2$ , of  $\eta$  itself. The value of  $\eta$  for niobium, which has a comparable  $T_c$  of 9 K, is in the range  $5.4\text{--}7.6 \text{ eV}/\text{\AA}^2$  [22]. However, in view of the uncertainties, not only in the frequency value, but the validity of Eq. (1) itself, this value of  $\lambda_{\text{e-ph}}$  cannot be expected to be more than a coarse approximation. It is known that even for one-component systems the rigid muffin-tin approximation usually gives values of the Hopfield parameter that are lower than those obtained via more rigorous calculations of the electron–phonon interaction (see Table II in Ref. [25]). For the solids under consideration with a large number of optical phonon branches, the extent

of underestimation is probably more severe. What is learnt from the above rigid muffin-tin (or atomic sphere) calculation is that the contribution to the electron–phonon coupling from both boron and palladium should be equally important, and that from the lithium atoms should be negligible.

Following the prescription of Gomersall and Gyorffy [15,16] one could try to analyse the electron–phonon coupling by writing

$$\lambda_{e-ph} = \lambda_{Pd} + \lambda_B = \frac{\eta_{Pd}}{M_{Pd}\langle\omega^2\rangle_{Pd}} + \frac{\eta_B}{M_B\langle\omega^2\rangle_B}, \quad (8)$$

where the subscripts Pd and B refer to atom-resolved quantities. This decomposition is based on the large difference between the Pd and B masses, and assumes that Li atoms do not contribute significantly to the electron–phonon coupling, as supported by the LMTO results. The heavy palladium atom vibration is assumed to couple to the electrons through zone boundary acoustic phonons and the lighter boron atom vibration is assumed to couple to electrons via the optical modes. It is reasonable to assume that in the acoustic modes only the palladium atoms vibrate, and in the optical modes only the lighter boron atoms vibrate. Instead of guessing the average phonon frequencies in the above equation, we can estimate the ratio  $\lambda_{Pd}/\lambda_B$  by assuming that the average optical phonon frequency is, to take an example, 2.5 times higher than the average zone boundary acoustic phonon frequency. With the values of  $\eta_{Pd}$  and  $\eta_B$  quoted in Table 2, we then find  $\lambda_{Pd} = 0.75\lambda_B$ , i.e. if the above scenario holds, then the boron contribution to the electron–phonon coupling is larger than the Pd contribution. For  $\lambda_{Pd}$  to be equal to or greater than  $\lambda_B$ , in this scenario, the average optical phonon frequency needs to be about 2.9 times or higher than the average zone boundary acoustic phonon frequency. From the consideration of the linear specific heat coefficient [26], Lee and Pickett [27] have obtained  $\lambda_{e-ph} = 0.74$ . With  $\lambda_{Pd} = 0.75\lambda_B$ , this would yield  $\lambda_{Pd} = 0.32$  and  $\lambda_B = 0.42$ . Note that the value  $\lambda_{Pd} = 0.32$  is not unreasonable, as a full-potential LMTO linear response calculation by Savrasov and Savrasov [28] yields  $\lambda_{Pd} = 0.35$  in elemental fcc Pd. Incidentally, the use of the McMillan expression [29]:

$$T_c = \frac{\Theta_D}{1.45} \exp \left\{ -\frac{1.04(1 + \lambda_{e-ph})}{\lambda_{e-ph} - \mu^*(1 + 0.62\lambda_{e-ph})} \right\}, \quad (9)$$

with the Coulomb pseudopotential  $\mu^*$  chosen to be 0.1, as it is often done,  $\Theta_D = 371$  K (Table 2), and  $\lambda_{e-ph} = 0.74$  yields  $T_c \sim 12$  K.

The above discussion points out that a description based on conventional (s-wave, spin singlet Cooper pairs) electron–phonon interaction should be applicable to  $\text{Li}_2\text{Pd}_3\text{B}$ . Of course a more rigorous calculation of the electron–phonon interaction is needed. Such a calculation is likely to reveal negligible coupling of lithium atom vibrations to the electron states at the Fermi level, while the vibrations of the palladium and boron atoms should couple strongly.

According to Yuan et al. [30] temperature dependence of the penetration depth in  $\text{Li}_2\text{Pd}_3\text{B}$  could be fit by a two-gap BCS model with a small (3.2 K) and a large (11.5 K) gap. Thus the claim is that  $\text{Li}_2\text{Pd}_3\text{B}$  is a two-gap BCS superconductor just like  $\text{MgB}_2$  [31–33]. The Fermi surface plots presented by Chandra et al. [4] show a Fermi surface with several sheets: a central large sheet and several smaller ones originating from the four bands crossing the Fermi level. A two or multi band superconductivity is thus conceivable in this material just as in  $\text{MgB}_2$  with two distinct sheets in the Fermi surface [34,35]. However,  $T_c$  may still be dominated by a single band [36], particularly in the absence of strong inter-band scattering.

### 3.2. $\text{Li}_2\text{Pt}_3\text{B}$ and the importance of SO coupling

The inadequacy of the above approach to describe the electron–phonon coupling in  $\text{Li}_2\text{Pt}_3\text{B}$  becomes clear from the much larger value of the Hopfield parameter obtained for this compound and listed in Table 2. Note that the unusually large contribution from boron is partly due to larger difference between the boron sphere radius  $s$  and the average Wigner–Seitz radius  $W$ . A calculation including empty spheres to reduce ASA errors would have changed the numbers in Table 2 somewhat, without changing the results qualitatively. Even with the reduced value of  $\Theta_D = 303$  K (Table 2), the much larger value of  $\eta$  would yield a value

for  $\lambda_{e-ph}$  larger than that for  $\text{Li}_2\text{Pd}_3\text{B}$ , implying a  $T_c$  that is actually higher than in  $\text{Li}_2\text{Pt}_3\text{B}$ . This is in clear contradiction to the experimental observation that  $T_c$  decreases monotonically as the Pt concentration increases from zero to unity.

The most serious drawback of the above analysis is the neglect of SO coupling, which is more pronounced in  $\text{Li}_2\text{Pt}_3\text{B}$  than in  $\text{Li}_2\text{Pd}_3\text{B}$ . SO coupling, in the absence of the center of inversion symmetry in these two compounds, can result in substantial splittings of the spin degenerate bands considered in this work. In a recent submission, Lee and Pickett [27] discuss SO coupled bands in both compounds: splitting of the spin degenerate bands is found to be as large as 30 meV and 200 meV at the Fermi level in  $\text{Li}_2\text{Pd}_3\text{B}$  and  $\text{Li}_2\text{Pt}_3\text{B}$ , respectively. The SO splitting of 30 meV or 348 K in  $\text{Li}_2\text{Pd}_3\text{B}$  is less than the estimated Debye temperature 371 K, the cut-off energy of the electron–phonon interaction. In  $\text{Li}_2\text{Pt}_3\text{B}$  the SO splitting is 200 meV or 2321 K, an order of magnitude larger than the estimated Debye temperature 303 K. It is clear that SO coupling would strongly alter the symmetry of the Cooper pairs, and the nature of the superconducting state in  $\text{Li}_2\text{Pt}_3\text{B}$  [13,37–39].

Yuan et al. [30] have claimed evidence of line of nodes in the energy gap in  $\text{Li}_2\text{Pt}_3\text{B}$ . Such a line of zeros in the energy gap is also seen in  $\text{CePt}_3\text{Si}$  [40], another noncentrosymmetric crystal with strong SO splitting of the spin degenerate bands [13]. The existence of the line of nodes is not a symmetry-imposed requirement and remains to be explained for both  $\text{Li}_2\text{Pt}_3\text{B}$  and  $\text{CePt}_3\text{Si}$ .  $\text{CePt}_3\text{Si}$  is a heavy fermion superconductor ( $T_c = 0.75$  K), so the mechanism of the pair formation is unclear.  $\text{Li}_2\text{Pt}_3\text{B}$  is most probably an electron–phonon superconductor, where the electron–phonon coupling needs to be determined from the SO coupled electron wavefunctions and is expected to differ strongly from that determined from the spin degenerate wavefunctions.

#### 4. Conclusions

The results presented in this work are not rigorous, and should only be used as a guide to under-

stand the relative strengths of coupling of the vibration of the different atoms to the electron states at the Fermi level. Based on these results, a description of superconductivity assuming conventional s-wave electron–phonon coupling and via a single electron–phonon coupling parameter appears possible in  $\text{Li}_2\text{Pd}_3\text{B}$ . The inclusion of SO coupling in the calculation of electron–phonon interaction should lead to improvement in results. For  $\text{Li}_2\text{Pt}_3\text{B}$  the SO effects are an order of magnitude stronger and do need to be included in the calculation of the electron–phonon interaction in order to explain the lower  $T_c$  in this compound.

The trends and the conclusions reached for  $\text{Li}_2\text{Pd}_3\text{B}$  in this work should be tested via rigorous calculation of the phonon frequencies and electron–phonon interaction. This is particularly important in view of the large number of phonon branches in this material. The results of this paper indicate that only the modes where the boron and the palladium atoms vibrate should couple to the electrons. The electron–phonon coupling should be equally strong for the modes where essentially the Pd atoms or the B atoms vibrate. According to our analysis the modes involving the vibrations of the Li atoms should show negligible coupling to electron states at the Fermi level. This is also suggested by our finding that almost the entire valence charge of lithium is transferred to the Pd–B complex (Section 2). Recent work of Lee and Pickett [27] also supports this conclusion. First principles linear response calculations of the phonons and electron–phonon coupling to verify the results of the present work are currently in progress.

Due to the strong SO coupling in  $\text{Li}_2\text{Pt}_3\text{B}$  the properties of the superconducting state is expected to deviate strongly from that described by spin-degenerate wavefunctions [13,37–39]. However, superconductivity should still be of the electron–phonon type (possibly also spin-singlet type, as suggested by Lee and Pickett [27]). The experimental result that  $T_c$  decreases monotonically in solid solutions  $\text{Li}_2\text{B}(\text{Pd}_{1-x}\text{Pt}_x)_3$  as the Pt concentration increases from zero to 1 indicates that the mechanism of electron pair formation remains unchanged, i.e. of the electron–phonon type.

## Acknowledgements

Financial support for this work was provided by Natural Sciences and Engineering Research Council of Canada. SKB gratefully acknowledges helpful discussion with O. Jepsen, B. Mitrović and K. V. Samokhin.

## References

- [1] U. Eibenstein, W. Jung, *J. Solid State Chem.* 133 (1997) 21.
- [2] K. Togano, P. Badica, Y. Nakamori, S. Orimo, H. Takeya, K. Hirata, *Phys. Rev. Lett.* 93 (2004) 247004.
- [3] P. Badica, T. Kondo, T. Kudo, Y. Nakamori, S. Orimo, K. Togano, *cond-mat/0404257*.
- [4] S. Chandra, S. Mathi Jaya, V.C. Valsakumar, *cond-mat/0502525*.
- [5] M. Sardar, D. Sa, *cond-mat/040168*.
- [6] M. Nishiyama, Y. Inada, G.-q. Zheng, *Phys. Rev. B* 71 (2005) 220505(R). *cond-mat/0506191 v1*.
- [7] T. Yokoya, T. Muro, I. Hase, H. Takeya, K. Hirata, K. Togano, *Phys. Rev. B* 71 (2005) 092507.
- [8] P. Badica, T. Kondo, K. Togano, *J. Phys. Soc. Jpn.* 74 (2005) 1014.
- [9] G.D. Gaspari, B.L. Gyorffy, *Phys. Rev. Lett.* 28 (1972) 801.
- [10] O.K. Andersen, *Phys. Rev. B* 8 (1975) 3060; O.K. Andersen, O. Jepsen, M. Sob, *Electronic structure and its applications*, in: M. Yossouff (Ed.), *Lecture Notes in Physics*, Springer, Berlin, 1987, pp. 1–57; O.K. Andersen, O. Jepsen, D. Glötzel, in: F. Bassani et al. (Eds.), *Highlights of Condensed Matter Theory*, North-Holland, Amsterdam, 1985, p. 59; H.L. Skriver, *The LMTO Method*, Springer, Berlin, 1984.
- [11] D. Glötzel, D. Rainer, H.R. Schober, *Z. Phys. B* 35 (1979) 317.
- [12] H.L. Skriver, I. Mertig, *Phys. Rev. B* 32 (1985) 4431.
- [13] K.V. Samokhin, E.S. Zijlstra, S.K. Bose, *Phys. Rev. B* 69 (2004) 094514; K.V. Samokhin, E.S. Zijlstra, S.K. Bose, *Phys. Rev. B* 70 (2004) 69902(E).
- [14] W.L. McMillan, *Phys. Rev.* 167 (1968) 331.
- [15] I.R. Gomersall, B.L. Gyorffy, *J. Phys. F* 3 (1973) L138.
- [16] B.M. Klein, D.A. Papaconstantopoulos, *Phys. Rev. Lett.* 32 (1974) 1193.
- [17] D.A. Papaconstantopoulos, B.M. Klein, *Phys. Rev. Lett.* 35 (1975) 110.
- [18] B.M. Klein, W.E. Pickett, D.A. Papaconstantopoulos, L.L. Boyer, *Phys. Rev. B* 27 (1983) 6721.
- [19] T. Jarlborg, A. Junod, M. Peter, *Phys. Rev. B* 27 (1983) 1558.
- [20] I.I. Mazin, S.N. Rashkeev, *Phys. Rev. B* 42 (1990) 366.
- [21] D. Rainer, *Prog. Low Temp. Phys.* X (1986) 371.
- [22] D.A. Papaconstantopoulos, L.L. Boyer, B.M. Klein, A.R. Williams, V.L. Moruzzi, J.F. Janak, *Phys. Rev. B* 15 (1977) 4221.
- [23] V.L. Moruzzi, J.F. Janak, K. Schwarz, *Phys. Rev. B* 37 (1988) 790.
- [24] C. Kittel, *Introduction to Solid State Physics*, seventh ed., John Wiley, 1996, p. 59.
- [25] S.K. Bose, O.V. Dolgov, J. Kortus, O. Jepsen, O.K. Andersen, *Phys. Rev. B* 67 (2003) 214518.
- [26] K. Togano, H. Takeya, unpublished results communicated to W.E. Pickett (*cond-mat/0507105 v1*).
- [27] K.-W. Lee, W.E. Pickett, *cond-mat/0507105 v1*.
- [28] S.Y. Savrasov, D.Y. Savrasov, *Phys. Rev. B* 54 (1996) 16487.
- [29] P.B. Allen, B. Mitrović, in: H. Ehrenreich, F. Seitz, D. Turnbull (Eds.), *Solid State Physics*, 37, Academic, New York, 1982, p. 1.
- [30] H.Q. Yuan, D. Vandervelde, M.B. Salamon, P. Badica, K. Togano, *cond-mat/0506771*.
- [31] S. Soma et al., *Nature (London)* 423 (2003) 65.
- [32] I.I. Mazin, V.P. Antropov, *Physica C* 385 (2003) 49.
- [33] B. Mitrović, *J. Phys. Condens. Matter* 16 (2004) 9013.
- [34] J. Kortus, I.I. Mazin, K.D. Belashchenko, V.P. Antropov, L.L. Boyer, *Phys. Rev. Lett.* 86 (2001) 4656.
- [35] Y. Kong, O.V. Dolgov, O. Jepsen, O.K. Andersen, *Phys. Rev. B* 64 (2001) 020501(R).
- [36] B. Mitrović, *Eur. Phys. J. B* 38 (2004) 451.
- [37] L.P. Gorkov, E.I. Rashba, *Phys. Rev. Lett.* 87 (2001) 037004.
- [38] P.A. Frigeri et al., *Phys. Rev. Lett.* 92 (2004) 097001.
- [39] I.A. Sergienko, S.H. Curnoe, *Phys. Rev. B* 70 (2004) 214510.
- [40] K. Izawa et al., *Phys. Rev. Lett.* 94 (2005) 197002.